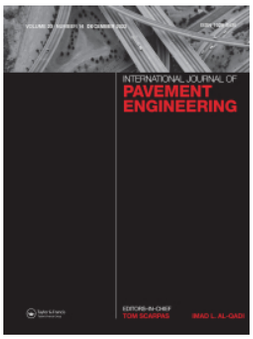

International Journal of Pavement Engineering

ISSN: (Print) (Online) Journal homepage: www.tandfonline.com/journals/gpav20

Influence of initial state and residual stresses on the modulus-density relationship of geomaterials: insights from multiple experimental setups

Amir Tophel, Troyee Tanu Dutta, Jeffrey P. Walker, Didier Bodin & Jayantha Kodikara

To cite this article: Amir Tophel, Troyee Tanu Dutta, Jeffrey P. Walker, Didier Bodin & Jayantha Kodikara (2024) Influence of initial state and residual stresses on the modulus-density relationship of geomaterials: insights from multiple experimental setups, International Journal of Pavement Engineering, 25:1, 2418920, DOI: 10.1080/10298436.2024.2418920

To link to this article: https://doi.org/10.1080/10298436.2024.2418920

Published online: 28 Oct 2024.

INTERNATIONAL JOURNAL OF PAVEMENT ENGINEERING
2024, VOL. 25, NO. 1, 2418920
https://doi.org/10.1080/10298436.2024.2418920

Taylor & Francis
Taylor & Francis Group

NOTE

Influence of initial state and residual stresses on the modulus-density relationship of geomaterials: insights from multiple experimental setups

Amir Tophel [a], Troyee Tanu Dutta [b], Jeffrey P. Walker [c], Didier Bodin [d] and Jayantha Kodikara [a]

[a]ARC Industrial Transformation Research Hub (ITRH) – SPARC Hub, Department of Civil Engineering, Monash University, Clayton, Australia; [b]Department of Civil Engineering, Indian Institute of Technology (IIT) Kharagpur, Kharagpur, India; [c]Department of Civil Engineering, Monash University, Clayton, Australia; [d]Australian Road Research Board (ARRB), Port Melbourne, Australia

ABSTRACT

Quality control in pavement construction traditionally relies on density measurements of geomaterials. With the introduction of modulus measurement methods, a shift has occurred due to the operational advantages of modulus-estimating devices over conventional density measurement techniques. Modulus-based methods also provide valuable information for the mechanistic-empirical (ME) design of pavement layers. However, a challenge emerges as a single modulus measurement does not directly correspond to a specific density measurement, leading to concerns about replacing density measurements in quality control processes. While it is generally accepted that a geomaterial's modulus primarily depends on its moisture content and density or void ratio, this study explores the complex relationship between modulus and density, particularly in field scenarios with consistent moisture content. Using three different laboratory-scale test set-ups, characterised by unique loading and boundary conditions, the research highlights the significant role of a geomaterial's initial state in obtaining accurate modulus estimates. The results reveal that identical densities can exhibit variations in modulus due to differences in initial densities and the development of residual lateral stresses. These variations in field conditions often stem from different paving or spreading techniques, emphasising the need for a comprehensive approach when establishing density-modulus correlations..

ARTICLE HISTORY
Received 18 March 2024
Accepted 14 October 2024

KEYWORDS
Modulus; lateral stress; initial state; void ratio; density

1. Introduction

During the construction of road pavement layers, geomaterials are compacted using rollers to achieve a target dry density or void ratio ensuring satisfactory performance over time. With the advancement of mechanistic-empirical (ME) pavement design and performance-based construction specifications, there is a growing interest in methods that quantify performance-related soil parameters, such as modulus and stiffness. Portable spot tests methods, including the lightweight deflectometer (LWD), Clegg Hammer, Briaud Compaction Device (BCD), static Plate Load Test (PLT) and the GeoGauge, have been developed to assess soil stiffness and moduli. These measurement devices take less time than traditional density measurement methods and are gaining increasing popularity (Look 2020). Recently, continuous control compaction (CCC), also termed as intelligent compaction (IC), has emerged. This technology outfits compactor with sensors, such as accelerometers and GPS, enabling measurement of parameters related to stiffness or modulus, referred to as intelligent compaction meter values (ICMVs), addressing the limitations of point-based measurement devices. Such advancements have spurred research into the correlation between modulus and density, with the aim of potentially eliminating the need for density measurement in the quality assurance of compacted geomaterial (Mooney and Rinehart 2007, Xu *et al.* 2012, Imran *et al.* 2018, Hu *et al.* 2020, Look 2020). However, the relationship between stiffness or modulus and post-compaction material properties (like density) has not been uniquely determined (Meehan *et al.* 2012, Lee *et al.* 2017, Wang *et al.* 2022), and the topic remains an active area of investigation. Previous studies have also indicated that the non-unique relationship between modulus and density can be attributed to variations in moisture content (Li *et al.* 2017, Tatsuoka *et al.* 2021).

This technical note reveals that even with constant moisture content, a non-unique relationship between modulus and density ($\rho_{d,N}$) or void ratio (e_N) exists due to variations in initial void ratios (e_0). This observation stems from a series of experiments conducted using three experimental setups: the extra-large wheel tracker test, constant peak stress 1-D test, and constant radial stiffness triaxial test. These experiments tested four different geomaterials under cyclic loads. The three test setups facilitate the measurement of various moduli types, reflecting the diverse moduli observed in field conditions. For example, the constant peak stress cyclic 1-D test gauges the plastic modulus of the geomaterial, whereas the extra-large wheel tracker test and constant radial stiffness triaxial test assess the elastic or unloading modulus pertinent to traffic loads on pavements.

CONTACT Amir Tophel amirtophel@gmail.com amir.tophel@monash.edu

2. Materials and test methods

Material behaviour subjected to repeated loading was studied in three different experimental setups. Each scenario provided a different perspective on the material behaviour and allowed the study of material properties during repeated loading.

2.1. Materials characterisation

The grain size distribution of the four materials used in this study is shown in Figure 1, with Table 1 listing their geotechnical properties.

study. For an in-depth exploration of the test and setup, refer to (Bodin *et al.* 2013).

During the constant load test, the geomaterials were compacted using a compaction foot and subjected to a load of 5 kN. The deformation during compaction was recorded using LVDTs attached to the bottom of the mould. In a previous study, the (Tophel *et al.* 2023) established a constitutive equation that can calculate the Youngs' or dynamic modulus of the geomaterial (E_G) based on the compactor's applied load (F) and other known parameters using

$$E_G = \frac{(H_0C_1)^{\frac{-2\beta}{1+\beta m}} exp\left(\frac{2\beta}{C_1(1+\beta m)} \times \frac{(e_0 - e_N)}{1+e_0}\right) \times \left(\frac{\pi LR}{F}\right) E_s(1-\nu_1^2)}{E_s - (H_0C_1)^{\frac{-2\beta}{1+\beta m}} exp\left(\frac{2\beta}{C_1(1+\beta m)} \times \frac{(e_0 - e_N)}{1+e_0}\right) \times \left(\frac{\pi LR}{F}\right) E_s(1-\nu_2^2)}, \quad (1)$$

2.2. Extra-large wheel tracker test

A prototype of the roller compactor, termed the extra-large wheel tracker test, was utilised to study material properties under a constant load (refer to Figure 2(a)). The examined material, an unbound granular material (UGM) also known as crushed rock with moderate fines, constitutes the base layer of a pavement and is designated as Material 1 in this

where ν_1 and ν_2 are the Poisson's ratio of the geomaterial and the cylindrical compactor, respectively, E_s is Young's modulus of the steel compactor, F is the load applied by the compactor, whereas L is the length of the compactor, R is the radius of the compactor; C_1, m, α and β are material model parameters. The void ratio e_N at cycle, N is calculated from the initial void ratio and height i.e. e_0

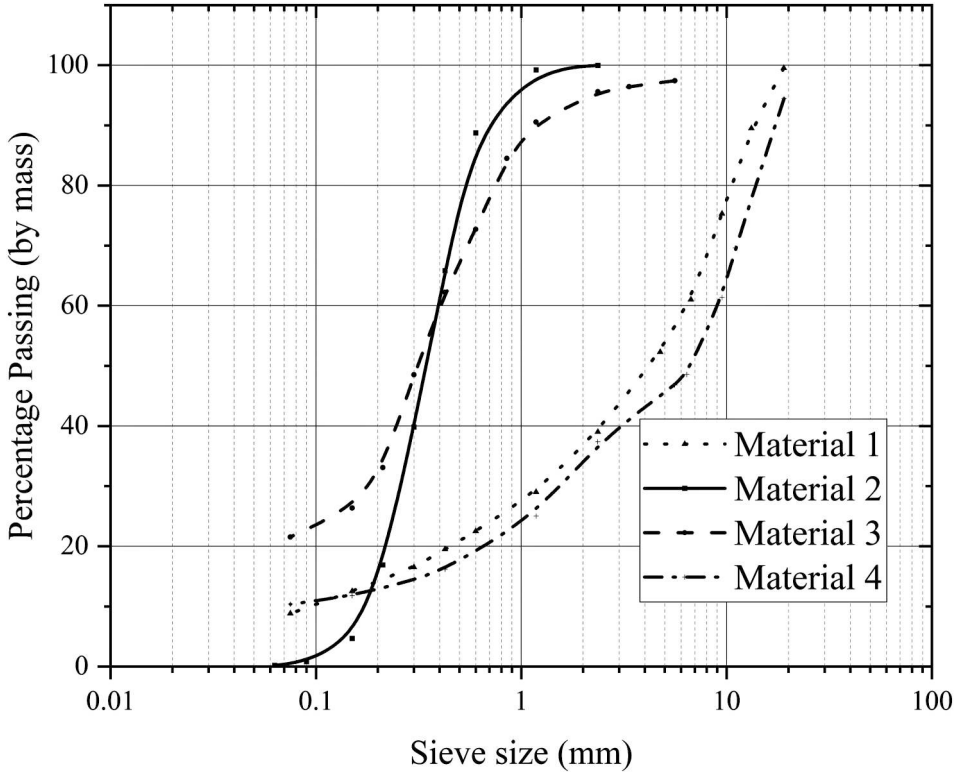

Figure 1. Grain size distribution of the four materials used in this study.

Table 1. Geotechnical properties of each material.

Material	Material 1	Material 2	Material 3	Material 4	Test Standard
Specific Gravity (G_s)	2.66	2.61	2.70	2.78	(ASTM D854 2002)
Optimum Moisture Content (OMC), modified Proctor (%)	6.6	9.3	8.0	5.8	(ASTM D1557-12E1 2003)
Maximum Dry Density (MDD), modified Proctor (t/m^3)	2.2	1.85	2.08	2.35	(ASTM D1557-12E1 2003)
Mean Particle Diameter (D_{50}) (mm)	4.5	0.45	0.32	6.5	(ASTM D6913/D6913M-17 2017)
Percentage passing the No. 200 sieve (%)	8.8	0.2	21	10	(ASTM D6913/D6913M-17 2017)
USCS Classification	GW	SC	SM	GW	(ASTM D2487-17 2017)

and H_0, respectively, using the deformation measured during compaction.

2.3. Constant peak stress cyclic 1-D test

The constant peak stress cyclic vibratory tests under 1-D conditions were conducted using a modified Proctor mould with dimensions of 150 mm in diameter and 150 mm in height, as shown in Figure 2(b). Compaction using a roller involves loading the sample up to 2 MPa of stress at around 18–30 Hz of vibratory loading (Mooney and Rinehart 2007, Rinehart and Mooney 2009, Tophel *et al.* 2022). In this study, a stress of 1120 kPa and vibration frequency of 18 Hz were selected based on the loading frame capacity. The test was performed on a sandy material, referred to as Material 2 in this study, at varying moisture content levels. This material typically constitutes a portion of the subgrade layer in the pavement cross-section. The modulus calculated in this study was plastic modulus (E_p) which is defined as the ratio of the vertical stress to the incremental plastic strain during the constant peak stress cyclic 1-D test compaction.

2.4. Constant radial stiffness triaxial test

A Constant Radial Stiffness Triaxial (CRST) test (Figure 2(c)) was then carried out on silty sand, a commonly used material for a pavement subbase and subgrade layer (named Material 3 in this study). To further validate the observations made for Material 3, a class 2 crushed rock, commonly used for the base layer of a pavement (named Material 4 in this study) was tested. A CRST test better represents pavement material behaviour under traffic loads by simulating dynamic confining pressures experienced in the field. Unlike traditional RLT tests with constant confining pressure, the CRST uses a rubber band to create a constant lateral stiffness boundary, allowing for realistic stress adjustments during cyclic loading. This approach facilitates increased radial stress and residual radial stress development, which is essential for achieving shakedown (Yu 2007, Dutta and Kodikara 2022). By better replicating real-world stress paths, the CRST test provides a more accurate assessment of pavement material performance under traffic conditions. In this instance, a modified version of Precision Unbound Material Analyser (PUMA) developed by The University of Nottingham and Cooper Research Technology is used (Li *et al.* 2017, Dutta and Kodikara 2022). The constant radial/lateral stiffness boundary condition was achieved using rubber bands that offered variable lateral stress conditions in the field. A stainless-steel band equipped with strain gauges was placed outside the rubber band to calculate the lateral strain in the band while the sample was loaded vertically. The circumferential strain in the band was used to compute the lateral strain and lateral stress on the soil sample using equations provided by (Dutta and Kodikara 2022). The applied vertical stress for tests on Material 3 was 360 kPa with a loading time of 0.1 sec and a rest time of 0.9 sec. The initial lateral stress (σ_{lat}) and stiffness (K_{lat}) used in these tests were approximately 10 kPa and 7 MPa respectively. In the case of Material 4 testing, the applied vertical stress was 500 kPa, while the other parameters were same as for Material 3. Material 3 is commonly used as a subbase and subgrade material, on the other hand, Material 4 is used as a base material; these specimens were tested at 360 and 500 kPa, respectively which replicates the typical load levels encountered due to traffic (AustRoads 2000).

Using the information of vertical and lateral stresses and strains, the resilient modulus of geomaterial (M_r) can be calculated using the equation provided by the European standard (EN 2004) as

$$M_r = \frac{(\sigma_{1,resilient})^2 + (\sigma_{1,resilient})(\sigma_{lat,resilient}) - 2(\sigma_{lat,resilient})^2}{(\sigma_{1,resilient})(\Delta\epsilon_{1,resilient}) + (\sigma_{lat,resilient})(\Delta\epsilon_{1,resilient}) - 2(\sigma_{lat,resilient})(\Delta\epsilon_{lat,resilient})}, \quad (2)$$

where $\sigma_{1,resilient}$, $\sigma_{lat,resilient}$ are the resilient stresses in the vertical and lateral directions due to the applied vertical stress, and $\Delta\epsilon_{1,resilient}$, $\Delta\epsilon_{lat,resilient}$ a the resilient strains in the axial/vertical and lateral directions, respectively.

3. Results and discussion

3.1. Influence of stress history and initial void ratio for constant load test

The incremental plastic deformation (ΔH_p) and incremental (average) plastic strain ($\Delta\epsilon_p$) variations of samples of Material 1 at a constant 4.13% gravimetric moisture content are plotted against void ratio at cycle number N (e_N), as shown in Figure 3(a) and (b), respectively. It can be observed that both parameters not only depend on the current void ratio (e_N), but also on the initial void ratio (e_0) of the sample. At a particular e_N, both parameters are lower for a higher initial void ratio. The small difference in the values of ΔH_p and $\Delta\epsilon_p$ corresponds to the difference in initial height of the samples.

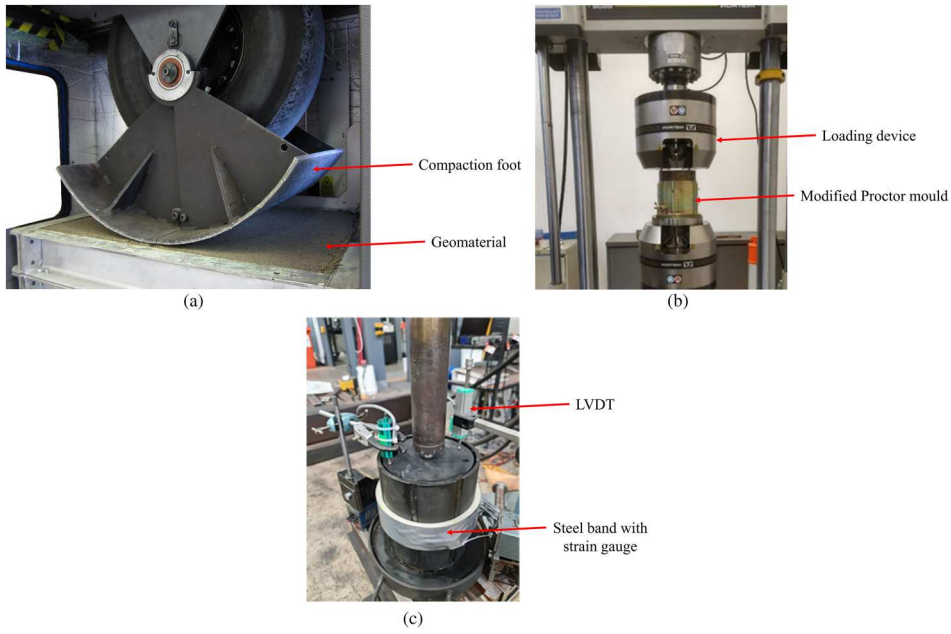

Figure 2. Experimental setup pictures: (a) extra-large wheel tracker apparatus; (b) constant peak stress cyclic 1-D test; and (c) constant radial stiffness triaxial test.

The non-unique relationships between ΔH_p and $\Delta\epsilon_p$ with e_N were also observed for geomaterial's Young's modulus (E_G), as shown in Figure 4, where the variation of E_G is plotted against void ratio. Although all the samples had the same moisture content (w), E_G was found to be dependent on e_0 of the sample and not unique for the same e_N or $\rho_{d,N}$. It should be noted that past research (Li and Selig 1994, Tatsuoka *et al.* 2021) also reported a non-unique relationship between density and modulus; however, the reason for this discrepancy is due to the difference in S_r. Referring to Figure 4, at a constant void ratio (which implies that the S_r is constant as w is constant), the E_G values were higher for samples compacted from a looser initial state or higher initial void ratio.

Figure 4 also illustrates the variation of Young's Modulus (E_G) with different initial void ratios for all six samples at a constant moisture content of 4.13%. Interestingly, the samples exhibit almost the same Young's Modulus at the start despite having different initial void ratios (0.373–0.590).

This observation can be attributed to all the samples having similar initial plastic strain, as demonstrated in Figure 3. The uniformity in initial plastic strain across samples with different void ratios leads to comparable modulus values.

3.2. Influence of stress history and initial void ratio for a constant peak stress cyclic test under K_0 condition

The constant stress test also exhibited a pattern similar to that observed in Figure 4. The modulus, plotted against the void ratio for samples of Material 2 at different moisture contents, indicated that a sample with a higher initial void ratio was stiffer than a sample with a lower initial void ratio. The tests conducted on different moisture contents revealed the dependence of material properties on moisture

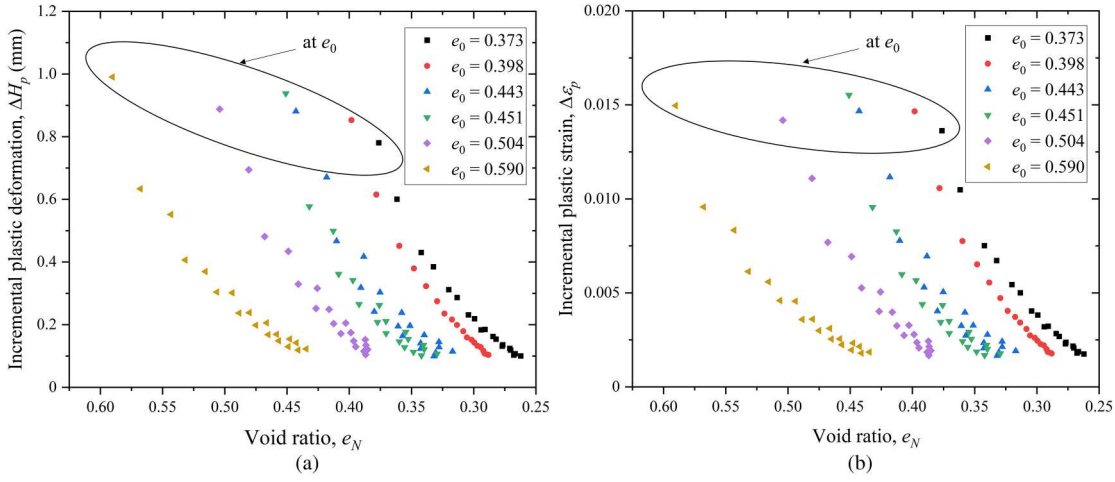

Figure 3. Variation of geomaterial properties with e_N: (a) ΔH_p, (b) $\Delta\epsilon_p$ at 4.13% moisture content for Material 1 in Extra-large wheel tracker test (constant load test).

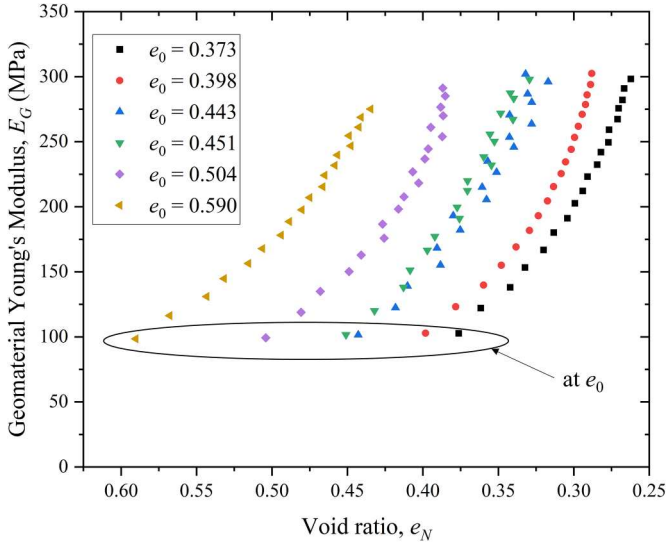

Figure 4. Variation of geomaterial's Young's modulus E_G with e_N for all six samples at 4.13% moisture content for Material 1 in Extra-large wheel tracker test (constant load test).

content, void ratio, and initial void ratio, as shown in Figure 5.

By closer inspection of Figure 4, it can be seen that samples exhibit significant differences in E_G values, which can be attributed to the wide range of initial void ratios (0.373–0.590). In contrast, Figure 5 does not show a drastic change in the modulus due to the limited variation in initial void ratios.

3.3. Influence of stress history and initial void ratio for CRST test

The CRST test showed similar behaviour for resilient modulus to the other two test setups (Figure 6(a)) for moisture content of 8% for Material 3. As stated before, the test setup allowed measurement of the lateral stress development during repeated cyclic loading which is shown in Figure 6(b).

Considering the same void ratio (e =0.336), the lateral stress values are 42 and 32 kPa for $e_0 = 0.389$ and $e_0 = 0.354$, respectively (as observed in Figure 6(b)). This

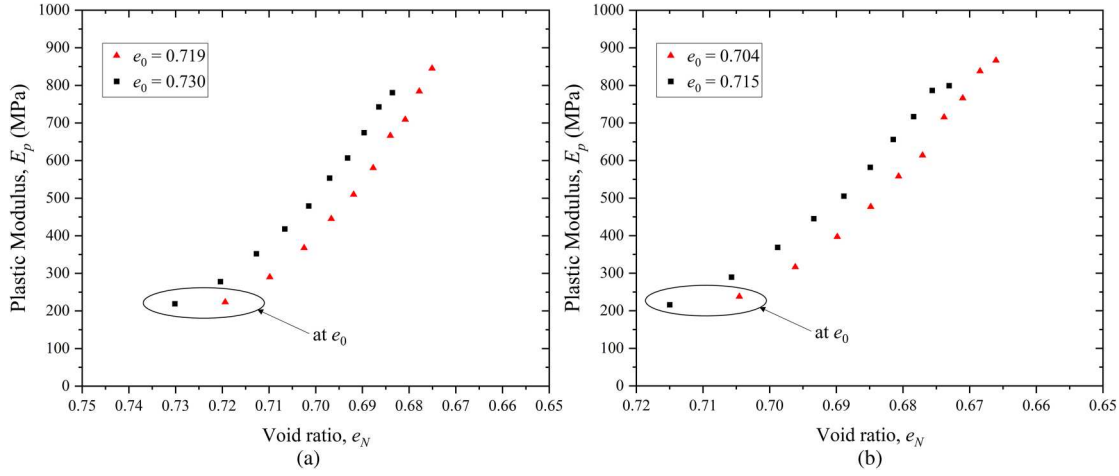

Figure 5. Variation of plastic modulus with the void ratio for (a) moisture content of 5% and (b) moisture content 7% for Material 2 in constant peak stress cyclic 1-D test.

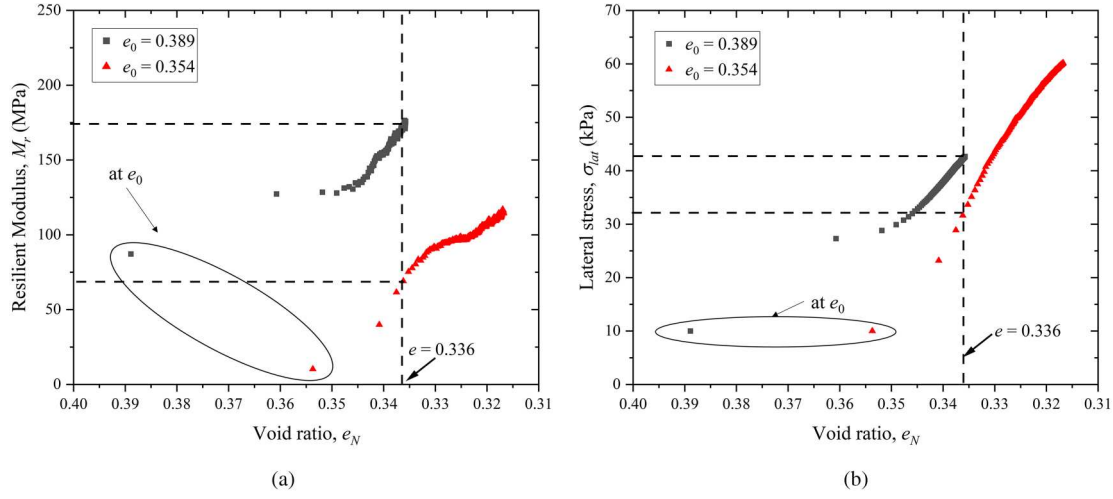

Figure 6. Variation of (a) resilient modulus with void ratio and (b) lateral stress with void ratio at 8% moisture content for Material 3 in constant radial stiffness triaxial test.

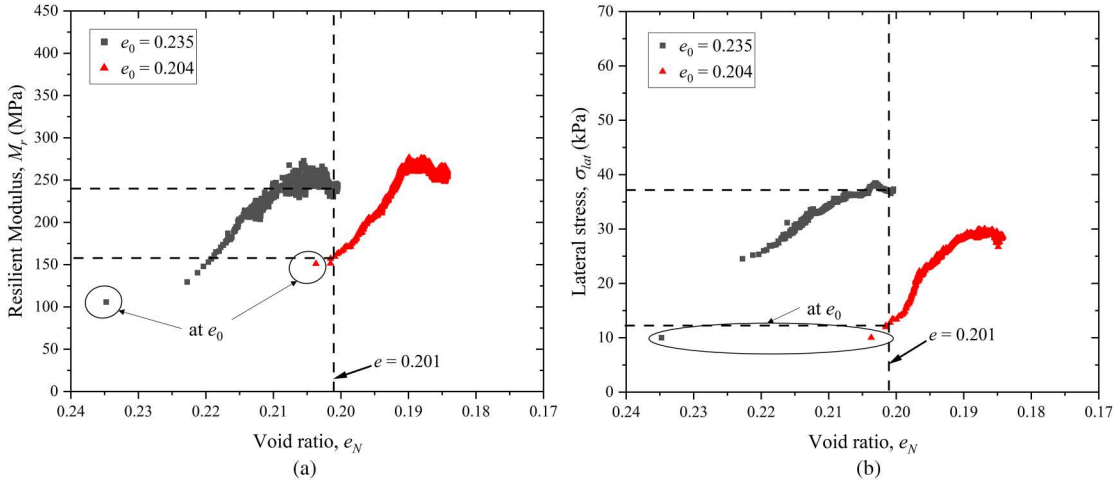

Figure 7. Variation of (a) resilient modulus with void ratio and (b) lateral stress with void ratio at 4.9% moisture content for Material 4 in constant radial stiffness triaxial test.

indicates that the sample with a higher initial void ratio undergo greater cumulative plastic deformation and therefore requires more cycles to reach a particular void ratio. This results in higher residual lateral stress development, which increases mean stress for specimens with higher e_0. This contributes to the higher resilient modulus value of 175 MPa compared to 70 MPa at the same void ratio/density of 0.336.

For Material 4, tested at a moisture content of 4.9%, the behaviour of modulus and lateral stress is illustrated in Figure 7. Similar to Material 3, the lateral stresses are higher for a sample having a higher initial void ratio giving rise to a higher resilient modulus at one particular void ratio. Considering void ratio, $e = 0.201$, the values of lateral stresses are 37 and 13 kPa for $e_0 = 0.235$ and $e_0 = 0.204$, respectively (From Figure 7(b)). The resilient modulus values are 240 MPa compared to 160 MPa for $e_0 = 0.235$ and $e_0 = 0.204$, respectively (From Figure 7(a)).

These observations can also be rationalised using the theoretical model proposed by Pestana and Whittle (1995), where the elastic bulk modulus (K) is expressed as a function of void ratio (e) and mean effective stress (p') as shown below:

$$K = K_0 p_a \left(\frac{1+e}{e}\right)\left(\frac{p'}{p_a}\right)^c, \tag{3}$$

$$p' = p + \chi s, \tag{4}$$

where K_0, c are fitting parameters, p_a is atmospheric pressure, p is mean net stress $\left(\frac{\sigma_1 + 2\sigma_3}{3}\right)$, s is suction, and χ is Bishop's parameter (Bishop 1959), which is considered equal to the degree of saturation (S_r) (Houlsby 1997, Borja 2006, Kuczmann and Iványi 2008, Coussy 2011, Manzanal *et al.* 2011). For a particular material with constant moisture and void ratio, the increase in p' is due to the increase in lateral stress (σ_3) in the sample as S_r remains the same. This increase in p' results in an increase in bulk modulus (K).

4. Conclusion

This study explored the relationship between modulus and density of geomaterials under varying initial conditions and loading setups, emphasizing the influence of initial void ratios and stress history on the resulting modulus values. Through three distinct experimental setups – the extra-large wheel tracker test, constant peak stress cyclic 1-D test, and constant radial stiffness triaxial (CRST) test – we examined the behaviour of four different materials.

Key findings from this study include:

1. Non-unique Relationship Between Modulus and Density:

It was observed that even with a constant moisture content, the modulus of a geomaterial is not uniquely related to its density. This non-uniqueness can be attributed to variations in the initial void ratios of the samples. The results demonstrated that identical densities can exhibit variations in modulus due to differences in initial compaction states and the subsequent development of residual lateral stresses.

2. Impact of Initial Void Ratios:

Samples with higher initial void ratios exhibited higher modulus values after compaction. This suggests that the initial state of the material significantly influences its final modulus. The development of residual lateral stresses during compaction plays a crucial role in this phenomenon, altering the mean stress and consequently the material's modulus.

3. Behaviour Under Different Loading Conditions:
The three test setups provided different perspectives on material behaviour. The extra-large wheel tracker test primarily assessed the elastic or unloading modulus pertinent to traffic loads. The constant peak stress cyclic 1-D test measured the plastic modulus, reflecting conditions similar to those experienced during roller compaction. The CRST test offered

insights into resilient modulus under traffic-like lateral confinement, better simulating field conditions.

4. Influence of Stress History and Lateral Confinement:
The CRST test highlighted the importance of lateral confinement in accurately representing pavement material behaviour under traffic loads. Maintaining constant radial stiffness more closely simulates the lateral confinement experienced in the field, providing a better understanding of how residual stresses and initial conditions affect modulus values.

5. Practical Implications for Pavement Construction:
The findings underscore the need to consider the initial state of the material when establishing correlations between density and modulus for quality control purposes. Variations in initial compaction conditions, as well as the resulting residual stresses, must be factored into any assessment of material performance.

In conclusion, this study provides valuable insights into the complex relationship between modulus and density, emphasizing the critical role of initial void ratios and stress history. These findings have significant implications for the mechanistic-empirical design and quality control of pavement layers, highlighting the need for comprehensive approaches that account for the initial state and stress conditions of geomaterials. Future research should continue to explore these relationships, particularly under varied field conditions, to further refine the understanding and application of modulus-based quality assurance methods in pavement construction.

Acknowledgments

The first author received a Monash University Graduate Scholarship (MGS) to undertake this research project. This research work was also part of a research project (Project No IH18.03.3) sponsored by the SPARC Hub (https://sparchub.org.au) at the Department of Civil Engineering, Monash University, funded by the Australian Research Council (ARC) Industrial Transformation Research Hub (ITRH) Scheme (Project ID: IH180100010). The authors would like to acknowledge the Australian Road Research Board (ARRB) for providing the experimental data and technical and in-kind support. The authors would also like to acknowledge Austroads for funding projects TT1611 and TT1819. The authors gratefully acknowledge the financial and in-kind support of Monash University, SPARC Hub, CIMIC, and EIC activities.

Disclosure statement

No potential conflict of interest was reported by the author(s).

Funding

This study was supported by the Australian Research Council (ARC) Industrial Transformation Research Hub (ITRH) Scheme (grant number IH180100010).

ORCID

Amir Tophel http://orcid.org/0000-0002-7478-2696
Troyee Tanu Dutta http://orcid.org/0000-0002-2378-2864
Jeffrey P. Walker http://orcid.org/0000-0002-4817-2712
Didier Bodin http://orcid.org/0000-0002-7314-6006
Jayantha Kodikara http://orcid.org/0000-0003-1725-7972

References

ASTM D1557-12E1, 2003. Standard test methods for laboratory compaction characteristics of soil using. *ASTM Standard Guide*, 3.
ASTM D2487-17, 2017. Standard practice for classification of soils for engineering purposes (Unified Soil Classification System). In *ASTM International*, West Conshohocken, PA, USA (Vols. D2487-17).
ASTM D6913/D6913M-17, 2017. Standard test methods for particle-size distribution (Gradation) of Soils Using Sieve Analysis 1. *ASTM International*.
ASTM D854, 2002. Standard test methods for specific gravity of soil solids by water pycnometer. *ASTM International*, 04.
AustRoads, 2000. *AG:PT/T053 Determination of permanent deformation and resilient modulus characteristics of unbound granular materials under drained conditions*.
Bishop, A.W., 1959. The principle of effective stress. *Teknik Ukeblad*, 39, 859–863.
Bodin, D., Moffatt, M., and Jameson, G., 2013. Development of a wheel-tracking test for rut resistance characterisation of unbound granular materials. *Austroads Publication*, AP-T240-13.
Borja, R.I., 2006. On the mechanical energy and effective stress in saturated and unsaturated porous continua. *International Journal of Solids and Structures*, 43 (6), 1764–1786. doi:10.1016/j.ijsolstr.2005.04.045.
Coussy, O., 2011. *Mechanics and physics of porous solids*. Chichester: John Wiley & Sons.
Dutta, T.T. and Kodikara, J., 2022. Evaluation of unbound/subgrade material rutting and resilient behaviour based on initial density and saturation degree. *Transportation Geotechnics*, 35, 100782. doi:10.1016/j.trgeo.2022.100782.
EN, B.S., 2004. 13286-7 (2004) unbound and hydraulically bound mixtures–cyclic load triaxial test for unbound mixtures. *British Standard Institute, UK*.
Houlsby, G.T., 1997. The work input to an unsaturated granular material. *Géotechnique*, 47 (1), 193–196. doi:10.1680/geot.1997.47.1.193.
Hu, W., *et al.*, 2020. Influence of moisture content on intelligent soil compaction. *Automation in Construction*, 113, 103141. doi:10.1016/j.autcon.2020.103141.
Imran, S.A., *et al.*, 2018. Artificial neural network-based intelligent compaction analyzer for real-time estimation of subgrade quality. *International Journal of Geomechanics*, 18 (6), 1–14. doi:10.1061/(ASCE)GM.1943-5622.0001089.
Kuczmann, M. and Iványi, A., 2008. *The finite element method in magnetics*. University College of Swansea, 308. https://www.researchgate.net/publication/265492483_The_Finite_Element_Method_in_Magnetics.
Lee, J., Lacey, D., and Look, B., 2017. *P60: Best practice in compaction QA for pavement and subgrade materials (year 1–2016/2017)*. www.nacoe.com.au.
Li, D. and Selig, E.T., 1994. Resilient modulus for fine-grained subgrade soils. *Journal of Geotechnical Engineering*, 120 (6), 939–957. doi:10.1061/(ASCE)0733-9410(1994)120:6(939).
Li, Q., Stein, J., and Garg, N., 2017. Characterization of airfield subbase materials using precision unbound material analyzer (PUMA), 370–381. doi:10.1061/9780784480939.032.
Look, B.G., 2020. Overcoming the current density testing impediment to alternative quality testing in earthworks. *Australian Geomechanics Journal*, 55 (1), 55–74.
Manzanal, D., Pastor, M., and Merodo, J.A.F., 2011. Generalized plasticity state parameter-based model for saturated and unsaturated soils. Part II: Unsaturated soil modeling. *International Journal for Numerical and Analytical Methods in Geomechanics*, 35 (18), 1899–1917. doi:10.1002/nag.983.
Meehan, C.L., Tehrani, F.S., and Vahedifard, F., 2012. A comparison of density-based and modulus-based in situ test measurements for compaction control. *Geotechnical Testing Journal*, 35 (3), 387–399. doi:10.1520/GTJ103479.
Mooney, M.A. and Rinehart, R.V., 2007. Field monitoring of roller vibration during compaction of subgrade soil. *Journal of Geotechnical and Geoenvironmental Engineering*, 133 (3), 257–265. doi:10.1061/(ASCE)1090-0241(2007)133:3(257).

Pestana, J.M. and Whittle, A.J., 1995. Compression model for cohesionless soils. *Géotechnique*, 45 (4), 611–631. doi:10.1680/geot.1995.45.4.611.

Rinehart, R.V. and Mooney, M.A., 2009. Measurement of roller compactor induced triaxial soil stresses and strains. *Geotechnical Testing Journal*, 32 (4), 101889. doi:10.1520/GTJ101889.

Tatsuoka, F., Hashimoto, T., and Tateyama, K., 2021. Soil stiffness as a function of dry density and the degree of saturation for compaction control. *Soils and Foundations*, 61 (4), 989–1002. doi:10.1016/j.sandf.2021.06.007.

Tophel, A., *et al*., 2022. Theory-guided machine learning to predict density evolution of sand dynamically compacted under Ko condition. *Acta Geotechnica*, 17 (8), 3479–3497. doi:10.1007/s11440-021-01431-2.

Tophel, A., *et al*., 2023. Model development to predict dynamic interactions of roller and geomaterial using simulated roller compaction. *Transportation Geotechnics*, 39, 100946. doi:10.1016/j.trgeo.2023.100946.

Wang, N., *et al*., 2022. Compaction quality assessment of cement stabilized gravel using intelligent compaction technology—A case study. *Construction and Building Materials*, 345, 128100. doi:10.1016/j.conbuildmat.2022.128100.

Xu, Q., Chang, G.K., and Gallivan, V.L., 2012. Development of a systematic method for intelligent compaction data analysis and management. *Construction and Building Materials*, 37, 470–480. doi:10.1016/j.conbuildmat.2012.08.001.

Yu, H.-S., 2007. *Plasticity and geotechnics*. Vol. 13. New York: Springer Science & Business Media.